ACS SENSORS

pubs.acs.org/acssensors

Article

Dual Methylation-Sensitive Restriction Endonucleases Coupling with an RPA-Assisted CRISPR/Cas13a System (DESCS) for Highly Sensitive Analysis of DNA Methylation and Its Application for Point-of-Care Detection

Xianfeng Wang, Shiying Zhou, Chengxiang Chu, Mei Yang, Danqun Huo,* and Changjun Hou*

Cite This: *ACS Sens.* 2021, 6, 2419−2428

Read Online

ACCESS | Metrics & More | Article Recommendations | Supporting Information

ABSTRACT: High-performance detection of DNA methylation possesses great significance for the diagnosis and therapy of cancer. Herein, for the first time, we present a digestion strategy based on dual methylation-sensitive restriction endonucleases coupling with a recombinase polymerase amplification (RPA)-assisted CRISPR/Cas13a system (DESCS) for accurate and sensitive determination of site-specific DNA methylation. This dual methylation-sensitive restriction endonuclease system selectively digests the unmethylated target but exhibits no response to methylated DNA. Therefore, the intact methylated DNA target triggers the RPA reaction for rapid signal amplification. In contrast, the digested unmethylated target initiates no RPA reaction. RPA products with a T7 promoter can execute the T7 transcription in the presence of T7 RNA polymerase to generate a large number of single-stranded RNA (ssRNA). This ssRNA can be recognized by CRISPR/Cas13a to induce the ssRNase activity of Cas13a, showing the indiscriminate cleavage of the collateral FQ reporter to release the fluorescence signal. With such a design, by combining the unique features of dual methylation-sensitive restriction endonucleases with RPA-assisted CRISPR/Cas13a, the DESCS system not only presents the rapid and powerful signal amplification for the determination of methylated DNA with ultrahigh sensitivity but also effectively eliminates the false positive influences from incomplete digestion of the unmethylated target. More importantly, 0.01% methylation level can be effectively distinguished with the existence of excess unmethylated DNA. In addition, the DESCS assay is integrated into the lateral flow biosensor (LFB) for the point-of-care determination of DNA methylation. In view of the superiorities in high sensitivity, outstanding selectivity, and ease of operation, the DESCS system will provide a reliable assay for site-specific analysis of methylation.

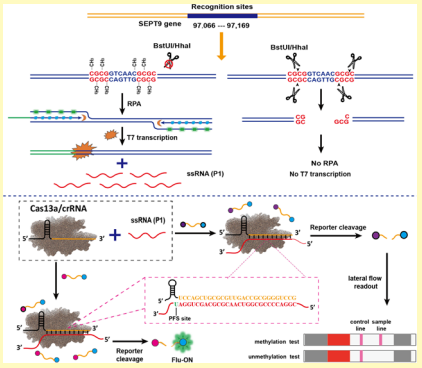

KEYWORDS: *DNA methylation, CRISPR/Cas, trans-cleavage, lateral flow biosensor, RPA, POCT*

DNA methylation is the most important epigenetic modification to cause a heritable change without any gene sequence change.[1] C5 methylation of cytosine at the CpG islands is the most common methylation that plays irreplaceable roles in regulating gene transcription, X-chromosome inactivation, and cell proliferation.[2,3] Customarily, most CpG islands in the promoter regions usually exhibit the unmethylated state, which ensures regular transcription initiation.[4] However, the promoter with CpG methylation exhibits a low initiation activity.[5] It is verified that the aberrant CpG methylation level in the regions of the gene promoter and the first exon is associated with the pathogenesis of multiple diseases, including cancer.[6,7] Therefore, the alterations of DNA methylation are deemed as a promising biomarker for early diagnosis, prognosis, and therapy monitoring of cancer.[8,9] In view of these, accurate and reliable determination of site-specific DNA methylation will provide great clinical relevance in disease diagnosis and pathological studies.

Currently, the strategy based on bisulfite conversion (BC) is deemed as the gold-standard methylation assay.[10,11] After reaction with sodium bisulfite, unmethylated cytosine (C) can be converted to uracil (U), whereas methylated cytosine exhibits no structural change.[12] Thus, the determination of methylated cytosine can be realized by distinguishing the architectural difference between uracil and methylcytosine.[13] Although the BC strategy provides outstanding performances in methylation detection, it still involves the disadvantages such as tedious pretreatment, a time-consuming process, requirement of multiple reagents, and extreme experimental conditions (eg., strong acid, strong alkaline, and high temperature).[14,15] To make

Received: April 3, 2021
Accepted: May 10, 2021
Published: May 21, 2021

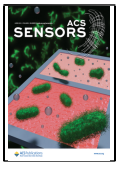

https://doi.org/10.1021/acssensors.1c00674
ACS Sens. 2021, 6, 2419−2428

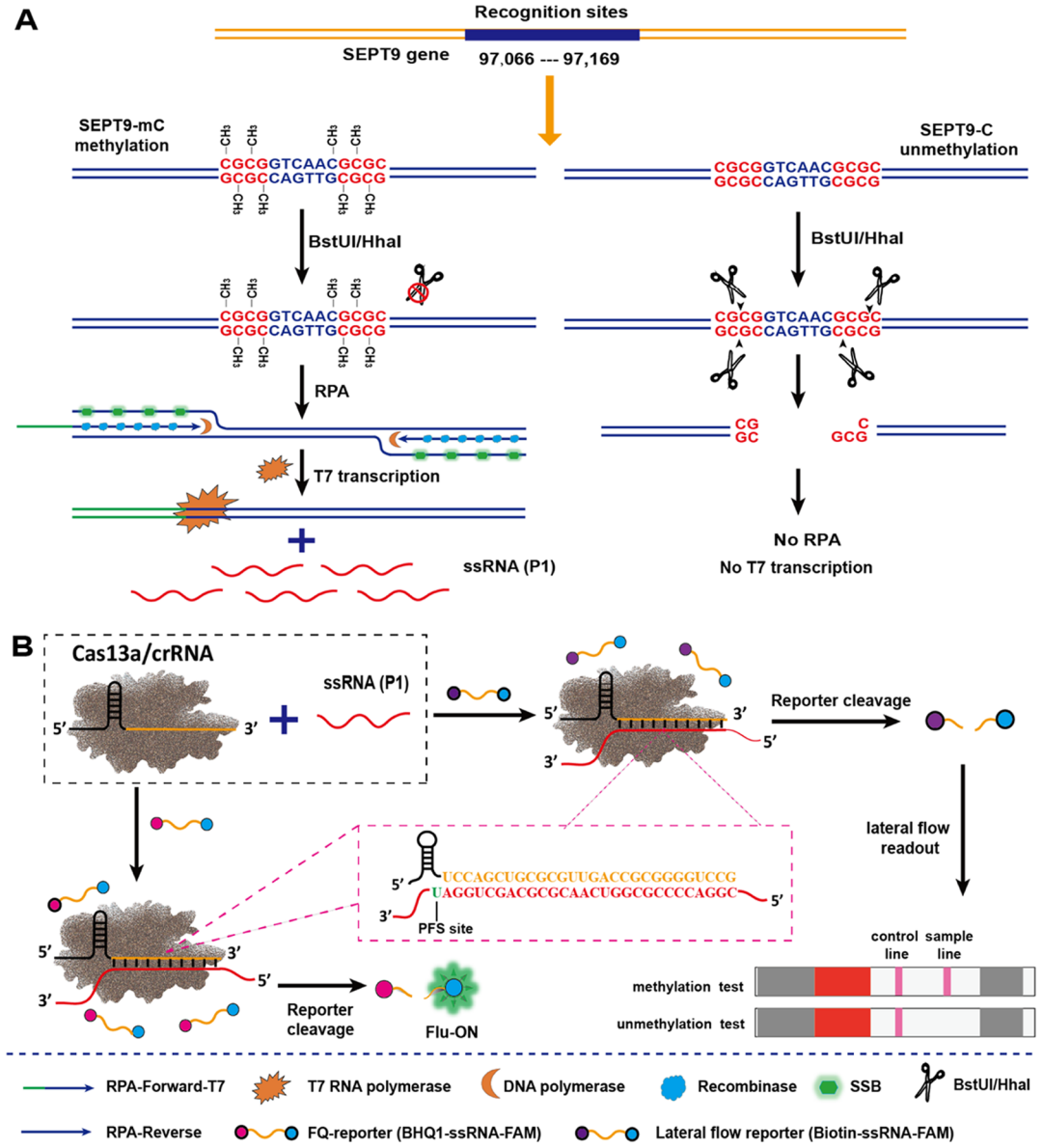

Figure 1. Schematic illustration of the DESCS strategy for the detection of DNA methylation. (A) Dual methylation-sensitive endonucleases system (*Bst*UI/*Hha*I) digests unmethylated DNA and leaves the methylated DNA intact. The intact methylated DNA triggers the subsequent RPA reaction and T7 transcription to generate ssRNA. (B) ssRNA products are recognized by the CRISPR/Cas13a system for cleavage of the FQ reporter to release the fluorescence signal. The DESCS assay is integrated into the lateral flow sensor for point-of-care detection of DNA methylation.

matters worse, the BC strategy suffers from target degradation, poor DNA recovery, and incomplete conversion,[16,17] which leads to the inaccurate measurement and the poor repeatability for methylation detection, especially for the low abundance of methylation. Therefore, it is urgent to explore bisulfite-free methods for methylation analysis.

The methylation-sensitive restriction endonuclease digestion (MRED) provides a bisulfite-free assay for DNA methylation detection. The endonuclease-based strategy shows the discrimination capacity of methylated and unmethylated DNA via the specific recognition capacity, which can be inhibited by the methylated restriction site.[18,19] The MRED-based strategies are executed in mild conditions, which reduces the potential DNA degradation and provides a rapid and facile operation.[20] In addition, multiple endonucleases are simultaneously applied to ensure the complete digestion of unmethylated DNA, which improves the accuracy and specificity of methylation analysis.[21]

Generally, methylated DNA from tumor cells exhibits a low existence (less than 0.1%) with the majority of unmethylated DNA in clinical samples.[22] Therefore, how to effectively detect DNA methylation from multitudinous unmethylated DNA is the key issue. To achieve enough sensitivity, different signal amplifications are always applied for methylation detection after endonuclease digestion. Among them, the polymerase chain reaction (PCR) is the most frequently employed technique for amplification in view of its excellent performances in sensitivity and accuracy.[23] Nevertheless, the PCR-based protocols heavily rely on the expensive and precise thermal cycling devices,[14] which limits their applications in real-time detection. As alternatives of PCR, several isothermal amplification methods, such as strand displacement amplification (SDA),[24] rolling circle amplification (RCA),[25,26] exponential amplification reaction (EXPAR),[27] and recombinase polymerase amplification (RPA),[28] have been presented for methylation analysis and

https://doi.org/10.1021/acssensors.1c00674
ACS Sens. 2021, 6, 2419−2428

effectively extricate the need of thermal cycles. However, the strategies based on SDA, RCA, and EXPAR exhibit poor competencies for double-stranded (dsDNA) amplification. In addition, SDA and RCA are time-consuming procedures, taking upwards of several hours to obtain amplification results and presenting relatively low sensitivity for methylation detection. In contrast, RPA has been proved as a promising means for effective signal amplification. The amplification reaction of dsDNA by RPA is performed under isothermal conditions (at lower temperatures of about 37−42 °C) with a mass of amplification products obtained within 20 min.[29] All of these advantages in economy, portability, and operability make RPA become an ideal method for real-time detection, especially in low-resource allocation.

Recently, the RNA-guided adaptive CRISPR/Cas systems have been altered as powerful diagnostic tools for diagnosis due to the discovery of trans-cleavage activity.[30] Among the Cas families, Cas12a, Cas12b, Cas13a, and Cas14 exhibit the indiscriminate digestion of surrounding ssDNA or ssRNA after specific recognition of target nucleic acids.[31,32] This trans-cleavage activity can be successfully employed to cleave the collateral FQ reporter with about thousands of turnovers per second, endowing these CRISPR/Cas systems with the specific capability of powerful self-signal amplification and reporting. Therefore, integrating CRISPR/Cas into the sensing system can indeed simplify the design procedures. The self-signal amplification of CRISPR/Cas coupling with other amplification strategies can easily obtain the multiple signal amplifications for sensing to provide excellent sensitivity. In addition, the nucleic acid recognition of CRISPR/Cas relies on a two-part model of crRNA and the Cas-enzyme. Only full complementation between target nucleic acid and the spacer region of crRNA can unlock the trans-cleavage of the Cas-enzyme, showing outstanding selectivity. Simultaneously, the programmability of crRNA makes CRISPR/Cas become a universal platform for any nucleic acid detection. To date, several CRISPR/Cas-based diagnostics versatile platforms, such as Cas13-based SHERLOCK,[33] Cas12-based HOLMES,[34] Cas12/Cas14-based DETECTR,[35,36] ASD-Cpf1,[37] and TITAC-Cas[38] have been exploited for isothermal determination of viruses (especially for COVID-19 diagnosis),[39] single nucleotide polymorphism (SNP), and non-nucleic acid targets with high sensitivity and selectivity, which also supports point-of-care testing (POCT) in vitro without the requirements of professional operator and instruments.[40,41] Therefore, it is a meaningful attempt to employ the CRISPR/Cas assay for DNA methylation analysis to achieve high sensitivity. As an attempt for exploration, Wang's group presented a HOLMESv2 strategy by integrating the CRISPR/Cas12b system with bisulfite conversion for the detection of DNA methylation.[42] After bisulfite treatment, the PCR products of methylated DNA can activate the trans-cleavage activity of the CRISPR/Cas12b system to release the fluorescence signal. The HOLMESv2 assay provides the potentials to broaden the applicable scopes for diverse detection. However, it still suffers from the disadvantages, such as high reaction temperature, the requirement of real-time PCR, and tedious treatments. Thus, alternative CRISPR/Cas assays are needed for the rapid detection of DNA methylation with simplicity of operator.

SEPT9 gene methylation is considered as an effective biomarker for colorectal cancer (CRC) screening and is the only cfDNA detection target approved in the clinic.[43−45] Therefore, we use the SEPT9 gene as an example to explore a new strategy for the detection of methylation biomarkers. Herein, we propose dual methylation-sensitive restriction endonucleases coupling with the RPA-assisted CRISPR/Cas13a system (DESCS) for highly sensitive analysis of SEPT9 gene methylation and its application for point-of-care detection. For DNA methylation detection, dual restriction-cutting sites are designed to ensure the complete digestion of unmethylated DNA. The target DNA with methylated restriction sites cannot be cleaved by these two restriction endonucleases and remain intact, which can be effectively amplified by the RPA reaction to obtain 10^6−10^9-fold amplification products within minutes. Of the methods explored, amplified DNA with a T7 promoter can be converted to a mass of ssRNA, which is recognized by the CRISPR/Cas13a system and triggers the trans-cleavage of Cas13a. As a result, the active CRISPR/Cas13a system executes the collateral cleavage of the FQ reporter to release the fluorescence signal. With such a design, site-specific CpG methylation in the SEPT9 gene is successfully determined by the DESCS assay in a 0.01% methylated sample with high sensitivity. In addition, the DESCS system is integrated into the CRISPR/Cas13a-based lateral flow sensor (LFB) to establish a rapid, reliable, and naked-eye platform for point-of-care detection of DNA methylation.

RESULTS AND DISCUSSION

Mechanism of RPA-Assisted CRISPR/Cas13a. The mechanism of the DESCS assay for the detection of site-specific methylation is expatiated in Figure 1, which integrates the advantages of high specificity of *Bst*UI/*Hha*I endonuclease for the digestion of unmethylated cytosine, and the powerful signal amplification efficiency of RPA and the CRISPR/Cas13a system. In this work, the SEPT9 gene containing the 5′-mCGmCG-3′/3′-GmCGmC-5′ site (97100 site) and the 5′-GmCGmC-3′/3′-mCGmCG-5′ site (97110 site) with 5-methylcytosine (mC) in the CpG island (referred to as "SEPT9-mC") serves as a site-specific methylation target, which exhibits the hypermethylation in human colorectal cancer. The unmethylated SEPT9 gene (referred to as "SEPT9-C") with the 5′-CGCG-3′/3′-GCGC-5′ (*Bst*UI) site and the 5′-GCGC-3′/3′-CGCG-5′ (*Hha*I) site are fully digested by *Bst*UI/*Hha*I endonucleases. Compared with single endonuclease digestion, this dual methylation-sensitive restriction endonucleases system provides a more powerful digestion capacity, which avoids the false-positive detection from incomplete digestion of unmethylated DNA. In contrast, the SEPT9-mC target cannot be recognized by the *Bst*UI/*Hha*I group and thus remain intact. Afterward, the intact SEPT9-mC target triggers the subsequent RPA reaction. Recombinase binds with the primer to search for the homologous sequence from the dsDNA target. Once the primer locates the homologous sequence, the SDA reaction is activated and the replaced DNA strand binds to the SSB to prevent further replacement. The RPA reaction generates a mass of dsDNA products conjugated with the T7 promoter. To realize the rapid detection, we integrate the subsequent T7 transcription and CRISPR/Cas13a recognition in one step. The RPA products can be converted to ssRNA by T7 transcription, which acts as the activator to induce the ssRNase activity of Cas13a, leading to the indiscriminate digestion of the RNA FQ reporter to release the fluorescence signal. Generally, RPA amplification unavoidably involves nonspecific amplification. The integration of transcription amplification and RNA recognition of CRISPR/Cas13 can effectively filter the background signal caused by DNA

https://doi.org/10.1021/acssensors.1c00674
ACS Sens. 2021, 6, 2419−2428

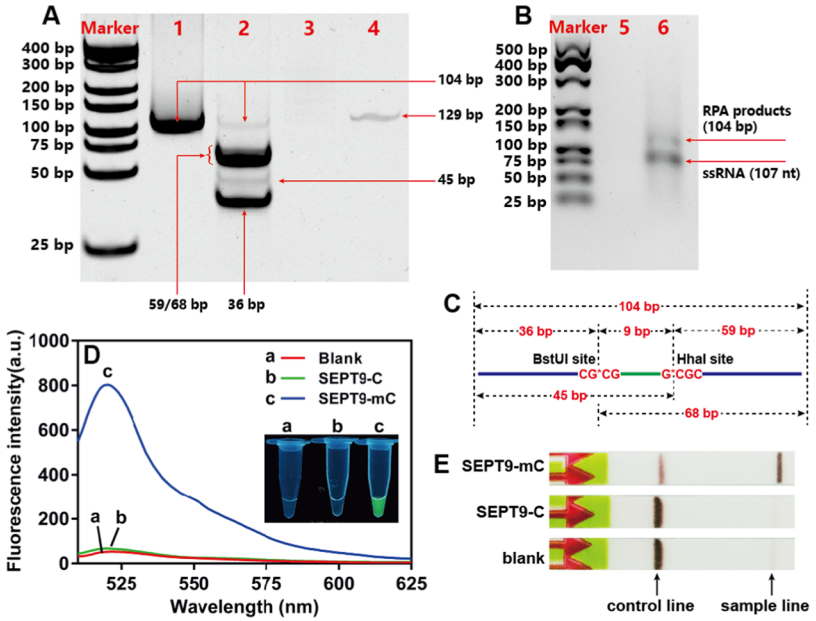

Figure 2. (A) Gel electrophoresis of digestion and the RPA reaction. Lane 1: methylated SEPT9-mC validation dsDNA + *Bst*UI/*Hha*I; lane 2: unmethylated SEPT9-C validation dsDNA + *Bst*UI/*Hha*I; lane 3: RPA products (with SEPT9-C target); and lane 4: RPA products (with SEPT9-mC target). (B) Agarose gel electrophoresis of T7 transcription. Lane 5: T7 transcription with unmethylated SEPT9-C; lane 5: T7 transcription with methylated SEPT9-mC. (C) Cleavage sites of *Bst*UI/*Hha*I and the length of digestion fragments for SEPT9 validation dsDNA. (D) Fluorescence spectra of different samples measured by the RPA-assisted CRISPR/Cas13a system: (a) Blank; (b) unmethylated SEPT9-C; (c) methylated SEPT9-mC. (E) Feasibility of DESCS-based lateral flow sensor for the detection of SEPT9-mC methylation.

nonspecific amplification. In addition, just by changing the FQ reporter to the lateral flow reporter, the DESCS assay can be integrated into a lateral flow sensor (LFB) to realize the point-of-care detection of DNA methylation.

Feasibility of DESCS Assay. To validate the powerful digestion capacity of the dual methylation-sensitive restriction endonucleases system, the methylated and unmethylated dsDNA with the full length (104 bp) of the recognition sequence were digested by *Bst*UI/*Hha*I. As can be seen from Figure 2A, several bands are obviously observed in lane 2. The back band with low electrophoretic mobility is related to the complete unmethylated dsDNA. Other bands with higher electrophoretic mobilities are corresponding to different digestion fragments (59/68, 45, and 26 bp). Since the 9 bp fragment is hard to be dyed, resulting in no appearance of the 9 bp-fragment band in lane 2. This is confirmed in Figure S1A. All of these digestions conform to the desired results exhibited in Figure 2C, demonstrating the site-specific digestion of the *Bst*UI/*Hha*I system. By comparison, only one band is observed in lane 1, which is assigned to the methylated dsDNA. This indicates that the *Bst*UI/*Hha*I system exhibits the methylation-sensitive features and the methylated dsDNA maintains the intact structure. Due to the interference from SSB and recombinase, the RPA products purified with the PCR purification kit were applied for gel electrophoresis analysis. An obvious band is observed from the SEPT9-mC sample in lane 4, which is coincident with the desired RPA products of methylated DNA. Notably, the unmethylated SEPT9-C sample presents no band in lane 3, indicating that the unmethylated SEPT9-C is digested by *Bst*UI/*Hha*I and leads to the RPA failure. Similarly, after T7 transcription, only the methylated SEPT9-mC sample can generate the ssRNA (107 nt), showing an obvious ssRNA band in lane 6 in Figure 2B. In contrast, the RPA failure of the unmethylated SEPT9-C sample leads to the nonperformance of T7 transcription. Therefore, no ssRNA band is observed in lane 5. To confirm the feasibility of the DESCS assay for methylated SEPT9-mC detection, RPA products were applied for T7 transcription amplification and CRISPR/Cas13a recognition. As can be seen from Figure 2D, methylated SEPT9-mC DNA induces a drastic fluorescence enhancement (curve c). In contrast, unmethylated SEPT9-C DNA presents the ignorable fluorescence enhancement (curve b) and exhibits a concordant fluorescence intensity with that of the blank group (curve a). All of these results suggest that the unmethylated SEPT9-C DNA is digested by a dual endonucleases system, which cannot initiate the subsequent RPA reaction, T7 transcription amplification, and CRISPR/Cas13a recognition. However, methylated SEPT9-mC DNA successfully triggers the RPA-assisted CRISPR/Cas13a system, suggesting that the DESCS assay can discriminate methylated SEPT9-mC from an unmethylated sample. For LFB detection, an obvious band is observed at the sample line for SEPT9-mC detection and the color of the control line fades, demonstrating that the methylated SEPT9-mC triggered the DESCS system to cleave the lateral flow reporter and the FAM/gold-NP-anti-FAM antibody is conjugated at the sample line. However, for the unmethylated SEPT9-C sample, only one band emerges at the control line, suggesting that the DESCS assay exhibits no response to unmethylated SEPT9-C DNA and the biotin-FAM/gold-NP-anti-FAM antibody is conjugated by streptavidin in the control line. All of these clearly indicate that the DESCS assay provides an undoubted feasibility for the determination of DNA methylation with high accuracy and sensitivity.

Optimization. To improve the detection performances, the experimental parameters, such as the concentration of *Bst*UI, *Hha*I, and T7 polymerase, and the response time of CRISPR/Cas13a were investigated. To achieve the rapid analysis of methylation, the digestion time was set as 1 h (30 min for *Bst*UI and 30 min for *Hha*I) to optimize the concentration of *Bst*UI and *Hha*I. To ensure complete digestion, an unmethylated

https://doi.org/10.1021/acssensors.1c00674
ACS Sens. 2021, 6, 2419−2428

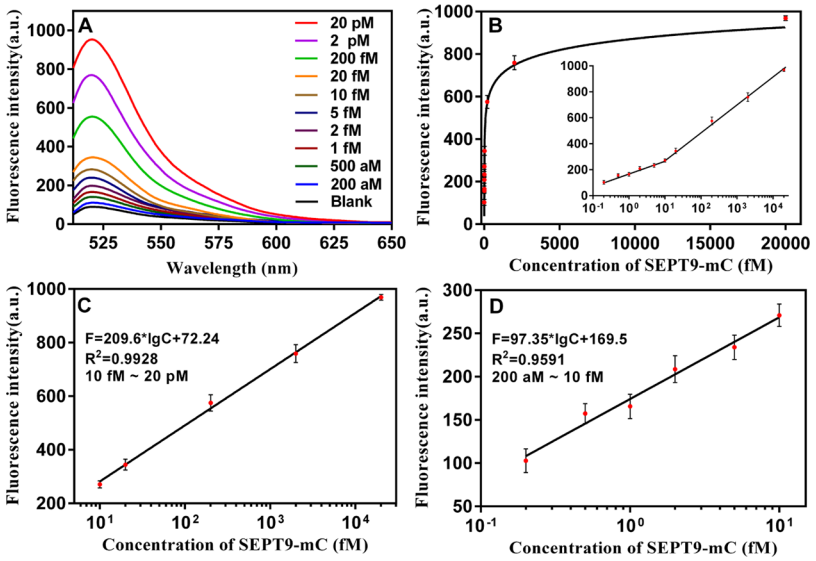

Figure 3. (A) Fluorescence spectra induced by various concentrations of methylated SEPT9-mC (20 pM, 2 pM, 200 fM, 20 fM, 10 fM, 5 fM, 2 fM, 1 fM, 500 aM, 200 aM, and blank). (B) Fluorescence response to different concentrations of methylated SEPT9-mC DNA at 520 nm. The corresponding logarithmic calibration curve in the linear range of 10 fM to 20 pM (C) and 200 aM to 10 fM (D).

Table 1. Comparison with Other Methods for Methylation Detection

method	signal amplification	detection range	LOD	ref
electrochemistry	tetrahedron RCA	1 fM to 10 nM	1 fM	46
electrochemistry	Fe_3O_4/TMC/Au nanocomposite and PT probe	100 fM to 5 nM	2 fM	47
electrochemistry	exonuclease III-assisted target recycling	10 fM to 100 pM	4 fM	48
SERS	Au NP-modified capture probe	5 pM to 5 nM	3 pM	49
colorimetry	antibody-MMPs/Au NPs	80 fM to 80 pM	80 fM	50
fluorescence	hyperbranched RCA	1 fM to 10 pM	0.8 fM	25
fluorescence	Fe@Au/dipyridamole probe	3.2 to 800 fM	0.31 fM	51
fluorescence	oxidation damage base-assisted amplification	100 fM to 100 nM	34.58 fM	52
fluorescence	upconversion nanoparticles/Au nanorods	10 pM to 100 nM	7 pM	53
fluorescence	dual endonucleases digestion coupling with RPA-assisted CRISPR/Cas13a	200 aM to 20 pM	86.4 aM	this work

substrate (SEPT9-C DNA) with a high concentration of 20 nM was applied for optimization. As depicted in Figure S2A, a strong fluorescence is observed without *Hha*I, while it gradually decreases with the growing concentration of *Hha*I. The fluorescence of the test sample is completely quenched at an *Hha*I concentration of 0.5 U·μL^{-1}, indicating that *Hha*I with a concentration of at least 0.5 U·μL^{-1} is needed for complete digestion of unmethylated DNA. Simultaneously, *Bst*UI also exhibits a concentration-dependent digestion of SEPT9-C DNA and a 0.2 U·μL^{-1} of *Bst*UI is selected as the minimum used concentration, which is lower than that of *Hha*I (Figure S2B). It demonstrates that *Bst*UI with the hot start characteristic exhibits a higher digestion efficiency compared with *Hha*I. In addition, the concentration of T7 RNA polymerase was also investigated. As shown in Figure S2C, the fluorescence response ($F - F_0$) depicts an increase with the growing concentration of T7 RNA polymerase and reaches the maximal value at 1.25 U·μL^{-1}. Therefore, 1.25 U·μL^{-1} of T7 RNA polymerase is selected as the optimal for methylation detection. To realize the rapid analysis, we present an improved integration strategy that T7 transcription and CRISPR/Cas13a recognition are performed in one step. The net fluorescence signal ($F - F_0$) of the DESCS system increases with the response time extension from 5 to 30 min. However, it shows the depressed response in the net fluorescence signal over 30 min (Figure S3D), which results from the nonspecific transcription and recognition. Thus, 30 min is chosen as the optimal detection time.

Detection Performances of the DESCS Assay. Different concentrations of methylated SEPT9-mC were measured using the DESCS assay under the optimal conditions. Figure 3A reveals the fluctuation of fluorescence intensity with the growing concentrations of SEPT9-mC, which increases with the growing concentrations of SEPT9-mC from 200 aM to 20 pM (Figure 3B). This indicates that the DESCS assay for SEPT9-mC methylation detection is a concentration-dependent process. The fluorescence response shows linear relationships with the logarithm of the concentration of SEPT9-mC DNA in the range of 200 aM to 10 fM (Figure 3C) and 10 fM to 20 pM (Figure 3D), respectively. Regression equations are described as $F = 209.6 \times \lg C + 72.24$ ($R^2 = 0.9928$) and $F = 97.35 \times \lg C + 169.5$ ($R^2 = 0.9591$), respectively. The detection of limit (LOD) is calculated as 86.4 aM (S/N = 3). Compared with other methods for methylation detection (Table 1), the DESCS assay provides a significant sensitivity and a wider linear range (about 6 orders of magnitude). All of these outstanding performances are guaranteed by the high efficiency of RPA amplification and T7 transcription amplification and the indiscriminate single-stranded RNase activity of Cas13a.

It is the critical indicator for the DESCS assay to discriminate the low abundance of methylated DNA with the existence of the massive unmethylated ingredient. Therefore, various mixtures

https://doi.org/10.1021/acssensors.1c00674
ACS Sens. 2021, 6, 2419−2428

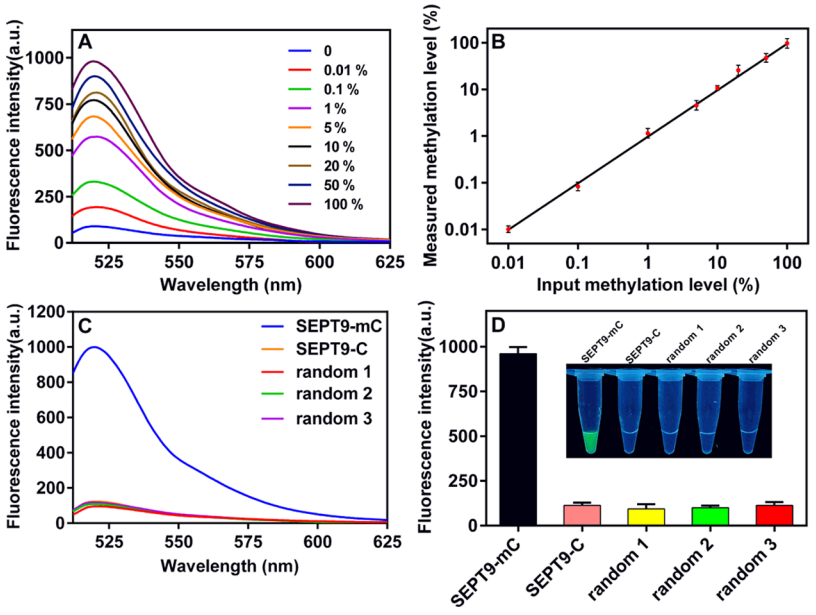

Figure 4. (A) Fluorescence spectra produced by the mixture of SEPT9-mC DNA and SEPT9-C DNA (total concentration of 20 pM). The ratios of SEPT9-mC DNA in the mixture are 0.01, 0.1, 1, 5, 10, 20, 50, and 100%, respectively. (B) Measured methylation level shows a good correlation with the actual input methylation level. (C) Fluorescence spectra induced by different DNA targets of methylated SEPT9-mC DNA, unmethylated SEPT9-C DNA, and random DNA. (D) Corresponding fluorescence response to different DNA targets.

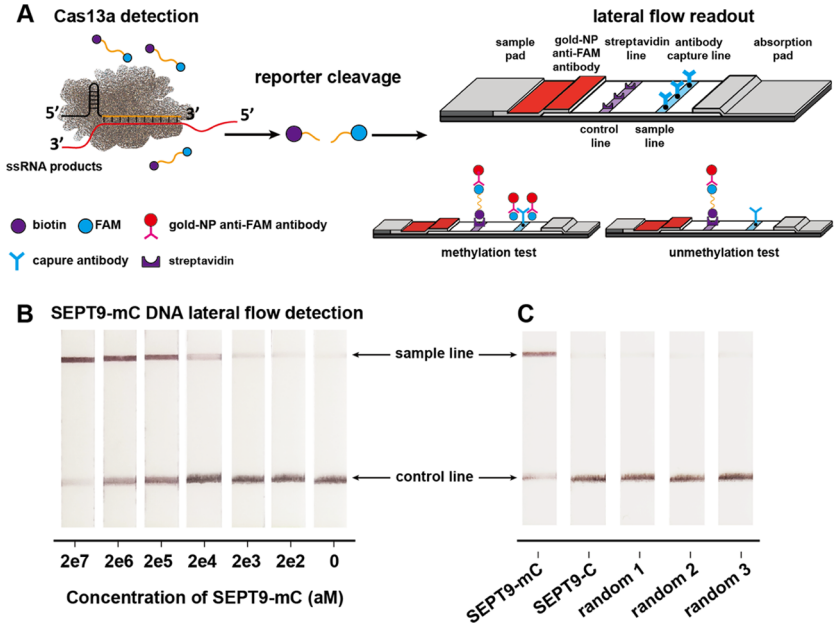

Figure 5. (A) Illumination of the DESCS-based LFB assay for methylation detection. (B) DESCS-based LFB responds to different concentrations of SEPT9-mC DNA. (C) DESCS-based LFB responds to different interferents.

composed of SEPT9-C and SEPT9-mC DNA were prepared with a total DNA concentration of 20 pM, in which the SEPT9-mC DNA possessed a ratio from 0.01 to 100% and subsequently tested by the DESCS assay. As seen from Figure 4A, the fluorescence intensity increases with the growing methylation levels of SEPT9-mC DNA from 0.01 to 100%. The measured methylation ratios show a linear relationship between the addition ratios of SEPT9-mC DNA (Figure 4B). The corresponding equation is described as: $Y = 0.9781 \times X - 0.0009781$. Notably, the 0.01% SEPT9-mC DNA (2 fM of methylated DNA) can be completely discriminated by the DESCS assay with the existence of mass unmethylated DNA, indicating the high selectivity and sensitivity of the DESCS assay for methylation detection. To further affirm the discrimination capability of the DESCS assay for site-specific methylation in the SEPT9 gene, the SEPT9-C DNA and other random DNAs were employed as the interferents and measured by the DESCS assay. As can be seen from Figure 4C,D, a distinct fluorescence enhancement (curve a and the black column) is observed in the existence of SEPT9-mC DNA. In contrast, the SEPT9-C DNA and three other interferents induce the negligible fluorescence signal. All of these results indicate that the DESCS assay presents an outstanding selectivity and discrimination capacity for DNA methylation detection, which results from the sequence-

https://doi.org/10.1021/acssensors.1c00674
ACS Sens. 2021, 6, 2419−2428

dependent recognition of CRISPR/Cas13a and the site-specific digestion capacity of the dual methylation-sensitive restriction endonuclease system. First, dual endonucleases of *Hha*I and *Bst*UI have the overlapping recognition sites of 5′-GCGC-3′. Thus, the dual methylation-sensitive restriction endonucleases system provides a more powerful digestion capacity than that of single endonuclease digestion, which is also demonstrated in the previous study.[20,54,55] In addition, the recognized sequence of CRISPR/Cas13a in the SEPT9 gene integrates two recognition sites (5′-GCGC-3′) of *Hha*I/*Bst*UI combination. Therefore, dual endonuclease digestion can effectively digest the crRNA recognition region so as to further avoid the background signal caused by nonspecific amplification.

Detection of DNA Methylation Using the LFB Assay. To obtain a naked-eye platform for point-of-care detection, the proposed method was integrated into the lateral flow sensor (DESCS-based LFB) for methylation analysis. Figure 5A reveals the sensing principle. Upon the existence of unmethylated or random DNA, the DESCS process cannot be executed and the CRISPR/Cas13a system maintains the inactive state. Thus, the lateral flow reporter (a short ssRNA labeled with 5′-FAM and 3′-Biotin) cannot be cleaved and remains intact, and all of the gold-NP-anti-FAM antibody binding with the intact lateral flow reporter is captured at the control line by the specific binding between biotin and streptavidin. In this case, only one brunet control band is observed. In contrast, the methylated DNA can trigger the RPA reaction and T7 transcription to generate a large number of ssRNA, which activates the trans-cleavage of the CRISPR/Cas13a system. The lateral flow reporter is cleaved into pieces. Therefore, the gold-NP-anti-FAM antibody just binding with FAM can be limited by the capture antibody at the test line, which presents two obvious bands for methylation detection. As shown in Figure 5B, the DESCS-based LFB shows the methylation-dependent gold-NP collection in the sample line. The sample line exhibits a gradual color change from colorless to dark with the growing concentrations of SEPT9-mC DNA. SEPT9-mC DNA with a low abundance of 200 aM can be obviously discriminated, indicating the ultrahigh sensitivity of the DESCS-based LFB assay. In addition, Figure 5C reveals that none of the tested interferents induced the colored band in the sample line, except for SEPT9-mC DNA, demonstrating the outstanding specificity of the DESCS-based LFB assay for methylation detection.

Analysis of DNA Methylation in Human Serum. Accurate measurement of DNA methylation in human serum possessed great meaning for the early diagnosis of tumor. To assess the real applications of the DESCS assay, different concentrations of SEPT9-mC DNA (0, 1, 10, 100 fM) were added to the 5% normal human serum and tested with the DESCS assay. As listed in Table S1, the acceptable results exhibit the recoveries from 91.3 to 96.9% with the RSD values ranging from 3.96 to 6.38%, indicating the validity of the DESCS assay for methylation detection in real applications.

CONCLUSIONS

In summary, the DESCS assay integrates dual methylation-sensitive restriction endonucleases (*Bst*UI/*Hha*I) coupling with an RPA-assisted CRISPR/Cas13a system for site-specific methylation detection of the SEPT9 gene. The DESCS assay integrates the advantages of high specificity and powerful digestion capacity of the *Bst*UI/*Hha*I system, and the incomparable amplification efficiency of RPA and the CRISPR/Cas13a system. With such a design, the DESCS assay presents an LOD as low as 86.4 aM for methylation detection with high selectivity. More importantly, the 0.01% methylation level can be effectively distinguished in a mixture of excess unmethylated DNA and trace unmethylated DNA. A DESCS-based lateral flow sensor is further established for point-of-care detection of DNA methylation with an eye-distinguishable concentration of 200 aM. Compared with other methods, the DESCS assay shows the advantages of ultrahigh sensitivity, outstanding selectivity, a low background signal, rapid operation, and naked-eye detection. In view of the programmability of crRNA, the DESCS assay can be further developed as a multiplexed platform for multiple target analysis.

EXPERIMENTAL SECTION

Reagents and Instruments. LwCas13a was purchased from Huicheng Reagent Company (Shanghai, China). CpG methyltransferase (M.SssI), *Hha*I endonuclease, *Bst*UI endonuclease, RNase Inhibitor (Murine), T7 RNA polymerase, RNA synthesis kit, rNTP, and dNTP were purchased from NEB (Beijing, China). The miRNA purification kit was ordered from TIANGEN (Beijing, China). The TS-GelRed dye was obtained from TSINGKE Co., Ltd. (Beijing, China). HybriDetect Dipstick (MGHD 1) was ordered from Milenia Biotec GmbH. The TwistAmp Basic kit for recombinase polymerase amplification (RPA) was ordered from TwistDx Limited (Maidenhead, U.K.). PAGE-related reagents were ordered from Coolaber Co., Ltd. SanPrep Column PCR Product Purification Kit, 1× TBE buffer (89 mM Tris, 89 mM boric acid, 2 mM EDTA, pH 8.3), 1× TE buffer (10 mM Tris−HCl, 1 mM EDTA, pH 7.4), DNA marker, PAGE-related reagents, 6× loading buffer (10 mM Tris−HCl, 60 mM EDTA, 40% bucrose, pH 7.6, 0.05% bromophenol blue, 0.05% xylene cyanol FF), and DNA probes used in this work were purchased from Sangon Biotech (China). The fluorescence spectra were recorded on a fluorescence spectrometer (PerkinElmer). All nucleic acid sequences involved in the present work are displayed in Table S2. The plasmid map of the PMD18-T-SEPT9 target is shown in Figure S3.

Preparation of crRNA. crRNA (64 nt) used in this work was synthesized by T7 transcription. A mixture containing T7-crRNA-F (10 μM) and T7 promoters (10 μM) was treated by denaturation (98 °C for 3 min) and a slow annealing process to form the transcription template. Then, 18 μL of transcription template, 10 μL of rNTP, and 2 μL of T7 RNA polymerase were fully mixed and incubated at 37 °C for 16 h. After that, the DNA template was digested by DNase I. The crRNA was purified with the miRNA purification kit and quantified by NanoDrop 2000C. The gel electrophoresis analysis of crRNA can be seen in Figure S4.

Preparation of CpG-Methylated Target. Unmethylated PMD18-T-SEPT9 target and SEPT9 validation dsDNA were treated by CpG methyltransferase (M.SssI) to obtain the CpG-methylated double-stranded SEPT9-mC DNA. Typically, 2 μg of unmethylated SEPT9 DNA was added to the mixture containing 10 μL of 10× NEBuffer 2.0 (500 mM NaCl, 100 mM Tris−HCl, 100 mM $MgCl_2$, 10 mM DTT, pH 7.9), 1 μL of *S*-adenosylmethionine (32 mM), 3 μL of M.SssI (4 U·μL^{-1}), and 86 μL of ddH_2O, and subsequently incubated at 37 °C for 5 h. To ensure exhaustive methylation, 3 μL of M.SssI (4 U·μL^{-1}) was further added and incubated for another 5 h. After that, the products were purified using the PCR product purification kit. The final CpG-methylated DNA was quantified with NanoDrop 2000C for further use.

Dual Endonucleases Digestion. Target DNA was digested by dual endonucleases treatment. It was carried out in a 20 μL of mixture containing 1× CutSmart buffer (50 mM potassium acetate, 20 mM Tris−acetate, 10 mM magnesium acetate, 100 μg/mL BSA, pH 7.9), 10 U of *Hha*I, 4 U of *Bst*UI, and a certain amount of target DNA. The mixture was reacted at 37 °C for 30 min and 60 °C for 30 min to ensure the complete digestion of the unmethylated target. After digestion, 0.5 μL of proteinase K (10 mg·mL^{-1}) was added and incubated at 60 °C for 15 min to inactivate *Hha*I and *Bst*UI.

https://doi.org/10.1021/acssensors.1c00674
ACS Sens. 2021, 6, 2419−2428

RPA-Assisted CRISPR/Cas13a Detection. For the RPA reaction, RPA pellets were dissolved in 29.5 μL of rehydration buffer to obtain the RPA solution. Then, 5.9 μL of RPA solution, 0.5 μL of RPA-forward primer (10 μM), 0.5 μL of RPA-reverse primer (10 μM), 1 μL of MgOAC solution (280 mM), and 2 μL of endonuclease-digested DNA sample were fully mixed and reacted at 42 °C for 25 min. CRISPR/Cas13a detection involves the T7 transcription amplification and product ssRNA-triggered RNase activity of Cas13a for trans-cleavage of the surrounding RNA FQ reporter. Typically, 2 μL of RPA product was added to 18 μL of a mixture containing 2 μL of 10× NEBuffer 2.1 (500 mM NaCl, 100 mM Tris−HCl, 100 mM $MgCl_2$, 1000 μg/mL BSA, pH 7.9), 1 U of RNase inhibitor, 2 μL of LwCas13a (0.5 μM), 2 μL of crRNA (2 μM), 2 μL of FQ reporter (10 μM), 25 U of T7 RNA polymerase, 0.8 μL of rNTP mix (25 mM), 0.5 μL of $MgSO_4$ (20 mM), and a certain amount of ddH_2O, which was subsequently incubated at 37 °C for 30 min. After that, 80 μL of RNase-free water was added and fluorescence spectra were recorded after the excitation of 480 nm. The operating procedure of lateral flow detection was concordant with the steps mentioned above, except that the RNA FQ reporter was replaced by the lateral flow reporter. The final reaction mixture was diluted 5 times with Hybridetect Assay Buffer. The HybriDetect strips were inserted into the reaction solution for 3 min. Then, the strips were taken out and photographed by a smartphone camera.

Gel Electrophoresis. The RPA-assisted CRISPR/Cas13a system for methylation detection was confirmed by PAGE analysis. In the RPA process, SSB and recombinase will bind with primers and other DNAs, which may improve DNA molecular weight and lead to unreliable electrophoresis results. Therefore, the RPA products must be purified before electrophoresis. The test sample was added to 1× loading buffer and then transferred into the lane of 15% polyacrylamide gel. Electrophoresis was performed in 1× TBE buffer at 110 V for 75 min. The final gel was dyed by 1× TS-GelRed and then photographed with a JENA UVsolo Imager.

Detection of CpG-Methylated DNA at Different Ratios. To confirm the specific determination capacity of the DESCS assay for the methylated DNA level in the complex sample, artificial mixtures with different ratios of methylated and unmethylated SEPT9 DNA were prepared. The total concentration of methylated SEPT9-mC DNA and unmethylated SEPT9-C DNA was set as 20 pM. Methylated PMD18-T-SEPT9-mC DNA existed in the mixture with a series of ratios of 0.01, 0.1, 1, 5, 10, 20, 50, and 100%. The measured methylation level was calculated according to the following equation

$$\text{methylation level}\ (\%) = \frac{M}{M+U} \times 100\%$$

where M represents the measured concentration of methylated SEPT9-mC DNA and U represents the unmethylated SEPT9-C DNA. Thus, $M + U = 20$ pM.

■ ASSOCIATED CONTENT

Supporting Information

The Supporting Information is available free of charge at https://pubs.acs.org/doi/10.1021/acssensors.1c00674.

Gel electrophoresis of digestion of SEPT9 validation dsDNA by *Bst*UI/*Hha*I; optimizations of experimental conditions; plasmid map of the PMD18-T-SEPT9 target; agarose gel electrophoresis of crRNA; real applications of the DESCS assay for methylation detection; and the DNA sequences used in this work (PDF)

■ AUTHOR INFORMATION

Corresponding Authors

Danqun Huo − *Key Laboratory for Biorheological Science and Technology of Ministry of Education, State and Local Joint Engineering Laboratory for Vascular Implants, Bioengineering College of Chongqing University, Chongqing 400044, P. R. China; Chongqing Key Laboratory of Bio-perception & Intelligent Information Processing, School of Microelectronics and Communication Engineering, Chongqing University, Chongqing 400044, P. R. China*; Phone: +86 23 6510 2507; Email: huodq@cqu.edu.cn

Changjun Hou − *Key Laboratory for Biorheological Science and Technology of Ministry of Education, State and Local Joint Engineering Laboratory for Vascular Implants, Bioengineering College of Chongqing University, Chongqing 400044, P. R. China; Chongqing Key Laboratory of Bio-perception & Intelligent Information Processing, School of Microelectronics and Communication Engineering, Chongqing University, Chongqing 400044, P. R. China*; orcid.org/0000-0002-2566-7165; Email: houcj@cqu.edu.cn

Authors

Xianfeng Wang − *Key Laboratory for Biorheological Science and Technology of Ministry of Education, State and Local Joint Engineering Laboratory for Vascular Implants, Bioengineering College of Chongqing University, Chongqing 400044, P. R. China*; orcid.org/0000-0002-7760-6647

Shiying Zhou − *Key Laboratory for Biorheological Science and Technology of Ministry of Education, State and Local Joint Engineering Laboratory for Vascular Implants, Bioengineering College of Chongqing University, Chongqing 400044, P. R. China*

Chengxiang Chu − *Key Laboratory for Biorheological Science and Technology of Ministry of Education, State and Local Joint Engineering Laboratory for Vascular Implants, Bioengineering College of Chongqing University, Chongqing 400044, P. R. China*

Mei Yang − *Key Laboratory for Biorheological Science and Technology of Ministry of Education, State and Local Joint Engineering Laboratory for Vascular Implants, Bioengineering College of Chongqing University, Chongqing 400044, P. R. China*; orcid.org/0000-0002-0062-605X

Complete contact information is available at: https://pubs.acs.org/10.1021/acssensors.1c00674

Author Contributions

X.W. and S.Z. contributed equally to this work. This manuscript was written through contributions of all authors. All authors have given approval to the final version of the manuscript.

Notes

The authors declare no competing financial interest.

■ ACKNOWLEDGMENTS

This work was supported by the National Natural Science Foundation of China (Nos. 81772290 and 81271930), the Graduate Scientific Research and Innovation Foundation of Chongqing, China (No. CYB20070,2020CDCGJ014), the Fundamental Research Funds for the Central Universities (2019CDYGZD007), the Higher Education Teaching Reform Research Project of Chongqing (203249), and the Chongqing Graduate Tutor Team Construction Project.

■ REFERENCES

(1) Goren, A.; Cedar, H. Replicating by the clock. *Nat. Rev. Mol. Cell Biol.* **2003**, *4*, 25−32.

(2) Reik, W.; Walter, J. Genomic imprinting: Parental influence on the genome. *Nat. Rev. Genet.* **2001**, *2*, 21−32.

(3) Choy, J. S.; Wei, S.; Lee, J. Y.; Tan, S.; Chu, S.; Lee, T.-H. DNA Methylation Increases Nucleosome Compaction and Rigidity. *J. Am. Chem. Soc.* **2010**, *132*, 1782−1783.

(4) De Smet, C.; Lurquin, C.; Lethé, B.; Martelange, V.; Boon, T. DNA Methylation Is the Primary Silencing Mechanism for a Set of Germ Line- and Tumor-Specific Genes with a CpG-Rich Promoter. *Mol. Cell. Biol.* **1999**, *19*, 7327−7335.
(5) Lee, E. J.; Luo, J.; Wilson, J. M.; Shi, H. Analyzing the cancer methylome through targeted bisulfite sequencing. *Cancer Lett.* **2013**, *340*, 171−178.
(6) Esteller, M.; Corn, P. G.; Baylin, S. B.; Herman, J. G. A gene hypermethylation profile of human cancer. *Cancer Res.* **2001**, *61*, 3225−3229.
(7) Rohde, C.; Zhang, Y.; Jurkowski, T. P.; Stamerjohanns, H.; Reinhardt, R.; Jeltsch, A. Bisulfite sequencing Data Presentation and Compilation (BDPC) web server - A useful tool for DNA methylation analysis. *Nucleic Acids Res.* **2008**, *36*, No. e34.
(8) Lofton-Day, C.; Model, F.; DeVos, T.; Tetzner, R.; Distler, J.; Schuster, M.; Song, X.; Lesche, R.; Liebenberg, V.; Ebert, M.; Molnar, B.; Grützmann, R.; Pilarsky, C.; Sledziewski, A. DNA methylation biomarkers for blood-based colorectal cancer screening. *Clin. Chem.* **2008**, *54*, 414−423.
(9) Laird, P. W.; Jaenisch, R. The role of DNA methylation in cancer genetics and epigenetics. *Annu. Rev. Genet.* **1996**, *30*, 441−464.
(10) Yuan, Y.; Hong, T.; Chen, Y.; Wang, Y.; Qiu, X.; Zheng, F.; Weng, X.; Zhou, X. Luminescence Sensing for Qualitative and Quantitative Detection of 5-Methylcytosine. *Anal. Chem.* **2018**, *90*, 10064−10068.
(11) Nesvet, J.; Rizzi, G.; Wang, S. X. Highly sensitive detection of DNA hypermethylation in melanoma cancer cells. *Biosens. Bioelectron.* **2019**, *124*−*125*, 136−142.
(12) Olek, A.; Oswald, J.; Walter, J. A Modified and Improved Method for Bisulphite Based Cytosine Methylation Analysis. *Nucleic Acids Res.* **1996**, *24*, 5064−5066.
(13) Wang, X.; Chen, F.; Zhang, D.; Zhao, Y.; Wei, J.; Wang, L.; Song, S.; Fan, C.; Zhao, Y. Single copy-sensitive electrochemical assay for circulating methylated DNA in clinical samples with ultrahigh specificity based on a sequential discrimination-amplification strategy. *Chem. Sci.* **2017**, *8*, 4764−4770.
(14) Sun, Y.; Sun, Y.; Tian, W.; Liu, C.; Gao, K.; Li, Z. A novel restriction endonuclease GlaI for rapid and highly sensitive detection of DNA methylation coupled with isothermal exponential amplification reaction. *Chem. Sci.* **2018**, *9*, 1344−1351.
(15) Wang, H.; Ke, H.; Zheng, Y.; Lai, J.; Luo, Q.; Chen, Q. A modified bisulfite conversion method for the detection of DNA methylation. *Epigenomics* **2017**, *9*, 955−969.
(16) Yi, S.; Long, F.; Cheng, J.; Huang, D. An optimized rapid bisulfite conversion method with high recovery of cell-free DNA. *BMC Mol. Biol.* **2017**, *18*, No. 24.
(17) Mouliere, F.; Chandrananda, D.; Piskorz, A. M.; Moore, E. K.; Morris, J.; Ahlborn, L. B.; Mair, R.; Goranova, T.; Marass, F.; Heider, K.; Wan, J. C. M.; Supernat, A.; Hudecova, I.; Gounaris, I.; Ros, S.; Jimenez-Linan, M.; Garcia-Corbacho, J.; Patel, K.; Ostrup, O.; Murphy, S.; Eldridge, M. D.; Gale, D.; Stewart, G. D.; Burge, J.; Cooper, W. N.; van der Heijden, M. S.; Massie, C. E.; Watts, C.; Corrie, P.; Pacey, S.; Brindle, K. M.; Baird, R. D.; Mau-Sorensen, M.; Parkinson, C. A.; Smith, C. G.; Brenton, J. D.; Rosenfeld, N. Enhanced detection of circulating tumor DNA by fragment size analysis. *Sci. Transl. Med.* **2018**, *10*, No. eaat4921.
(18) Melnikov, A. A.; Gartenhaus, R. B.; Levenson, A. S.; Motchoulskaia, N. A.; Levenson, V. V. MSRE-PCR for analysis of gene-specific DNA methylation. *Nucleic Acids Res.* **2005**, *33*, No. e93.
(19) Ramsahoye, B. H.; Burnett, A. K.; Taylor, C. Restriction endonuclease isoschizomers Ital, BsoFI and Fsp4HI are characterised by differences in their sensitivities to CpG methylation. *Nucleic Acids Res.* **1997**, *25*, 3196−3198.
(20) Wu, Z.; Bai, Y.; Cheng, Z.; Liu, F.; Wang, P.; Yang, D.; Li, G.; Jin, Q.; Mao, H.; Zhao, J. Absolute quantification of DNA methylation using microfluidic chip-based digital PCR. *Biosens. Bioelectron.* **2017**, *96*, 339−344.
(21) Liu, Y.; Wu, H.; Zhang, W.; Zhang, H.; Chen, H.; Zhou, G.; Gu, Y. Endonuclease-assisted hydrogel bead array for digital analysis of circulating tumor DNA methylation. *Sens. Actuators, B* **2020**, *304*, No. 127381.
(22) Diehl, F.; Li, M.; Dressman, D.; He, Y.; Shen, D.; Szabo, S.; Diaz, L. A., Jr.; Goodman, S. N.; David, K. A.; Juhl, H.; Kinzler, K. W.; Vogelstein, B. Detection and quantification of mutations in the plasma of patients with colorectal tumors. *Proc. Natl. Acad. Sci. U.S.A.* **2005**, *102*, 16368−16373.
(23) Kristensen, L. S.; Mikeska, T.; Krypuy, M.; Dobrovic, A. Sensitive melting analysis after real time-methylation specific PCR (SMART-MSP): High-throughput and probe-free quantitative DNA methylation detection. *Nucleic Acids Res.* **2008**, *36*, No. e42.
(24) Zhu, C.; Wen, Y.; Peng, H.; Long, Y.; He, Y.; Huang, Q.; Li, D.; Fan, C. A methylation-stimulated DNA machine: an autonomous isothermal route to methyltransferase activity and inhibition analysis. *Anal. Bioanal. Chem.* **2011**, *399*, 3459−3464.
(25) Cao, A.; Zhang, C.-y. Sensitive and Label-Free DNA Methylation Detection by Ligation-Mediated Hyperbranched Rolling Circle Amplification. *Anal. Chem.* **2012**, *84*, 6199−6205.
(26) Zeng, Y. P.; Hu, J.; Long, Y.; Zhang, C. Y. Sensitive detection of DNA methyltransferase using hairpin probe-based primer generation rolling circle amplification-induced chemiluminescence. *Anal. Chem.* **2013**, *85*, 6143−6150.
(27) Van Ness, J.; Van Ness, L. K.; Galas, D. J. Isothermal reactions for the amplification of oligonucleotides. *Proc. Natl. Acad. Sci. U.S.A.* **2003**, *100*, 4504−4509.
(28) Yin, K.; Ding, X.; Li, Z.; Zhao, H.; Cooper, K.; Liu, C. Dynamic Aqueous Multiphase Reaction System for One-Pot CRISPR-Cas12a-Based Ultrasensitive and Quantitative Molecular Diagnosis. *Anal. Chem.* **2020**, *92*, 8561−8568.
(29) Hice, S. A.; Clark, K. D.; Anderson, J. L.; Brehm-Stecher, B. F. Capture, Concentration, and Detection of Salmonella in Foods Using Magnetic Ionic Liquids and Recombinase Polymerase Amplification. *Anal. Chem.* **2019**, *91*, 1113−1120.
(30) Wang, M.; Zhang, R.; Li, J. CRISPR/cas systems redefine nucleic acid detection: Principles and methods. *Biosens. Bioelectron.* **2020**, *165*, No. 112430.
(31) Li, Y.; Li, S.; Wang, J.; Liu, G. CRISPR/Cas Systems towards Next-Generation Biosensing. *Trends Biotechnol.* **2019**, *37*, 730−743.
(32) Aquino-Jarquin, G. CRISPR-Cas14 is now part of the artillery for gene editing and molecular diagnostic. *Nanomedicine* **2019**, *18*, 428−431.
(33) Gootenberg, J. S.; Abudayyeh, O. O.; Kellner, M. J.; Joung, J.; Collins, J. J.; Zhang, F. Multiplexed and portable nucleic acid detection platform with Cas13, Cas12a, and Csm6. *Science* **2018**, *360*, 439.
(34) Li, S.-Y.; Cheng, Q.-X.; Wang, J.-M.; Li, X.-Y.; Zhang, Z.-L.; Gao, S.; Cao, R.-B.; Zhao, G.-P.; Wang, J. CRISPR-Cas12a-assisted nucleic acid detection. *Cell Discovery* **2018**, *4*, No. 20.
(35) Chen, J. S.; Ma, E.; Harrington, L. B.; Da Costa, M.; Tian, X.; Palefsky, J. M.; Doudna, J. A. CRISPR-Cas12a target binding unleashes indiscriminate single-stranded DNase activity. *Science* **2018**, *360*, 436−439.
(36) Harrington, L. B.; Burstein, D.; Chen, J. S.; Paez-Espino, D.; Ma, E.; Witte, I. P.; Cofsky, J. C.; Kyrpides, N. C.; Banfield, J. F.; Doudna, J. A. Programmed DNA destruction by miniature CRISPR-Cas14 enzymes. *Science* **2018**, *362*, 839−842.
(37) Wang, X.; Chen, X.; Chu, C.; Deng, Y.; Yang, M.; Ji, Z.; Xu, F.; Huo, D.; Luo, Y.; Hou, C. Four-stage signal amplification for trace ATP detection using allosteric probe-conjugated strand displacement and CRISPR/Cpf1 trans-cleavage (ASD-Cpf1). *Sens. Actuators, B* **2020**, *323*, No. 128653.
(38) Wang, X.; Zhou, S.; Chu, C.; Yang, M.; Huo, D.; Hou, C. Target-induced transcription amplification to trigger the trans-cleavage activity of CRISPR/Cas13a (TITAC-Cas) for detection of alkaline phosphatase. *Biosens. Bioelectron.* **2021**, *185*, No. 113281.
(39) Huang, Z.; Tian, D.; Liu, Y.; Lin, Z.; Lyon, C. J.; Lai, W.; Fusco, D.; Drouin, A.; Yin, X.; Hu, T.; Ning, B. Ultra-sensitive and high-throughput CRISPR-powered COVID-19 diagnosis. *Biosens. Bioelectron.* **2020**, *164*, No. 112316.

https://doi.org/10.1021/acssensors.1c00674
ACS Sens. 2021, 6, 2419−2428

(40) He, Q.; Yu, D.; Bao, M.; Korensky, G.; Chen, J.; Shin, M.; Kim, J.; Park, M.; Qin, P.; Du, K. High-throughput and all-solution phase African Swine Fever Virus (ASFV) detection using CRISPR-Cas12a and fluorescence based point-of-care system. *Biosens. Bioelectron.* **2020**, *154*, No. 112068.
(41) van Dongen, J. E.; Berendsen, J. T. W.; Steenbergen, R. D. M.; Wolthuis, R. M. F.; Eijkel, J. C. T.; Segerink, L. I. Point-of-care CRISPR/Cas nucleic acid detection: Recent advances, challenges and opportunities. *Biosens. Bioelectron.* **2020**, *166*, No. 112445.
(42) Li, L.; Li, S.; Wu, N.; Wu, J.; Wang, G.; Zhao, G.; Wang, J. HOLMESv2: A CRISPR-Cas12b-Assisted Platform for Nucleic Acid Detection and DNA Methylation Quantitation. *ACS Synth. Biol.* **2019**, *8*, 2228−2237.
(43) Li, J.; Zhou, X.; Liu, X.; Ren, J.; Wang, J.; Wang, W.; Zheng, Y.; Shi, X.; Sun, T.; Li, Z.; Kang, A.; Tang, F.; Wen, L.; Fu, W. Detection of Colorectal Cancer in Circulating Cell-Free DNA by Methylated CpG Tandem Amplification and Sequencing. *Clin. Chem.* **2019**, *65*, 916−926.
(44) Pan, Y.; Liu, G.; Zhou, F.; Su, B.; Li, Y. DNA methylation profiles in cancer diagnosis and therapeutics. *Clin. Exp. Med.* **2018**, *18*, 1−14.
(45) Powrózek, T.; Krawczyk, P.; Kucharczyk, T.; Milanowski, J. Septin 9 promoter region methylation in free circulating DNA—potential role in noninvasive diagnosis of lung cancer: preliminary report. *Med. Oncol.* **2014**, *31*, No. 917.
(46) Liu, H.; Luo, J.; Fang, L.; Huang, H.; Deng, J.; Huang, J.; Zhang, S.; Li, Y.; Zheng, J. An electrochemical strategy with tetrahedron rolling circle amplification for ultrasensitive detection of DNA methylation. *Biosens. Bioelectron.* **2018**, *121*, 47−53.
(47) Daneshpour, M.; moradi, L. S.; Izadi, P.; Omidfar, K. Femtomolar level detection of RASSF1A tumor suppressor gene methylation by electrochemical nano-genosensor based on Fe3O4/TMC/Au nanocomposite and PT-modified electrode. *Biosens. Bioelectron.* **2016**, *77*, 1095−1103.
(48) Feng, Q.; Qin, L.; Wang, M.; Wang, P. Signal-on electrochemical detection of DNA methylation based on the target-induced conformational change of a DNA probe and exonuclease III-assisted target recycling. *Biosens. Bioelectron.* **2020**, *149*, No. 111847.
(49) Hu, J.; Zhang, C.-y. Single base extension reaction-based surface enhanced Raman spectroscopy for DNA methylation assay. *Biosens. Bioelectron.* **2012**, *31*, 451−457.
(50) Ge, C.; Fang, Z.; Chen, J.; Liu, J.; Lu, X.; Zeng, L. A simple colorimetric detection of DNA methylation. *Analyst* **2012**, *137*, 2032−2035.
(51) Dadmehr, M.; Hosseini, M.; Hosseinkhani, S.; Ganjali, M. R.; Khoobi, M.; Behzadi, H.; Hamedani, M.; Sheikhnejad, R. DNA methylation detection by a novel fluorimetric nanobiosensor for early cancer diagnosis. *Biosens. Bioelectron.* **2014**, *60*, 35−44.
(52) Zhang, Y.; Li, C.-c.; Zhang, X.; Xu, Q.; Zhang, C.-y. Development of Oxidation Damage Base-Based Fluorescent Probe for Direct Detection of DNA Methylation. *Anal. Chem.* **2020**, *92*, 10223−10227.
(53) Wu, M.; Wang, X.; Wang, K.; Guo, Z. Sequence-specific detection of cytosine methylation in DNA: Via the FRET mechanism between upconversion nanoparticles and gold nanorods. *Chem. Commun.* **2016**, *52*, 8377−8380.
(54) Liu, Y.; Wu, H.; Zhang, W.; Zhang, H.; Chen, H.; Zhou, G.; Gu, Y. Endonuclease-assisted hydrogel bead array for digital analysis of circulating tumor DNA methylation. *Sens. Actuators, B* **2020**, *304*, No. 127381.
(55) Abe, M.; Kagara, N.; Miyake, T.; Tanei, T.; Naoi, Y.; Shimoda, M.; Shimazu, K.; Kim, S. J.; Noguchi, S. Highly sensitive detection of sentinel lymph node metastasis of breast cancer by digital PCR for RASSF1A methylation. *Oncol. Rep.* **2019**, *42*, 2382−2389.

https://doi.org/10.1021/acssensors.1c00674
ACS Sens. 2021, 6, 2419−2428